This item was submitted to Loughborough's Institutional Repository (https://dspace.lboro.ac.uk/) by the author and is made available under the following Creative Commons Licence conditions.

creative commons

COMMONS DEED

Attribution-NonCommercial-NoDerivs 2.5

You are free:

- to copy, distribute, display, and perform the work

Under the following conditions:

Attribution. You must attribute the work in the manner specified by the author or licensor.

Noncommercial. You may not use this work for commercial purposes.

No Derivative Works. You may not alter, transform, or build upon this work.

- For any reuse or distribution, you must make clear to others the license terms of this work.
- Any of these conditions can be waived if you get permission from the copyright holder.

Your fair use and other rights are in no way affected by the above.

This is a human-readable summary of the Legal Code (the full license).

Disclaimer

For the full text of this licence, please go to:
http://creativecommons.org/licenses/by-nc-nd/2.5/

Modelling the sputtering of Au surfaces using a multi time scale technique

Chris Scott and Roger Smith*

Department of Mathematical Sciences,

Loughborough University, Loughborough LE11 3TU, UK

(Dated: November 5, 2012)

Abstract

We present results from an atomistic computer simulation model of the sputtering of gold crystal surfaces under 500 eV ion bombardment by Au and Ar ions for doses up to 10^{14} ions.cm^{-2}. The multi time scale technique uses molecular dynamics to calculate the fast ballistic collision processes in the early stages of the cascade while an on-the fly kinetic Monte Carlo technique is used to model the relaxation and diffusion processes between successive ion impacts when the defect motion has begun to be dominated by rare events. The results indicate a large amount of crystalline recovery between impacts, some facetting of the crystal surfaces but no large sub-surface defect accumulation. Because of this recovery process, sputtering yields and energy distributions are in good agreement with those obtained assuming a perfect crystal surface and also with those experimentally measured.

PACS numbers: 46.05.+b,47.10.A-,79.20.Rf,81.16.Rf

Keywords: sputtering, long time scale dynamics, surface topography

*E-mail: R.Smith@lboro.ac.uk

1. INTRODUCTION

Since its discovery by Grove (Grove 1852), sputtering of surfaces by ion bombardment has been a topic which has many important applications and as such has been the subject of many books and research papers, (see e.g. the volumes edited by Behrisch (Behrisch 1981). A volume of the Philosophical Transactions of the Royal Society (Thompson et al 2004) published to celebrate the 150th anniversary of its discovery included applications associated with surface analysis, thin film growth by magnetron sputtering and dry etching, besides a number of theoretical and computer simulation articles. Sputtering continues to be an important area of research with an increasing number of technological applications, especially as a cost effective way for producing thin film coatings.

The first reported computer simulation of sputtering was in 1959 (Goldman et al 1959) using a Monte Carlo binary collision (BC) method and later in the 1960s classical molecular dynamics (MD) was used (Harrison 1960, Harrison et al 1966). Since that time there have been many applications of the MD technique to sputtering of complex systems (Postawa et al 2005, Webb et al 2011) while advances in analytical theory (Thompson 1968, Sigmund 1969), have been limited because of the linear cascade assumption and the difficulty of tailoring the models to specific molecular systems. By linear cascades we mean that atoms interact via binary collisions and not through multiple interactions. This is the basis of Boltzmann transport theory and computer codes such as TRIM or SRIM, (Ziegler, Biersack and Littmack, 1985).

MD computer models also have limitations and have difficulty in reaching experimental time scales thus many simulations have been carried out only by the analysis of individual atomic trajectories rather than an investigation of sequential impacts. This is because the maximum time step that can be used in the numerical integration of the equations of motion of N atoms is of the order of 1 fs (10^{-15}s). Thus even for small N the task of reaching laboratory time scales for typical ion beam currents by MD alone is computationally infeasible.

During the early stages of an MD simulation of an ion impact, atoms move about through ballistic collisions until their energy becomes shared by other atoms in the system (equipartition of energy). For a solid the atoms become trapped and then vibrate in metastable states. After this stage the system evolves more slowly due to rare events where an atom or group of atoms occasionally move together, hopping between these states. When this occurs a method other

than MD would be more appropriate to use. For example, if after the ballistic phase of the sputtering impact, the lowest energy barrier for a transition to occur was 0.3 eV, this event would be expected to occur on the time scale of 1 ns at 300K so we would have to perform $\approx 10^6$ MD steps to see the first transition. This problem is a general problem of MD and not unique to sputtering; for example it is also important in chemical reaction theory and the study of radiation effects. These slower events correspond to jumps over saddle points between local minima on the $3N$ dimensional potential energy surface so the key to bridging the time scales is to determine these transition pathways in a time efficient way.

Authors have tried to overcome the time scale problem in a number of ways. The simplest approach is to try to guess the likely transitions and incorporate these into a pre-determined list which is used in a kinetic Monte Carlo simulation. This is generally unsatisfactory since many important transitions can be missed but the method has had some success in modelling defect evolution in bulk metals (Domain et al, 2004). Other approaches is artificially increasing the dose rates (Yastrebov and Smith 2001) or running MD simulations at a higher temperature than the experiment to enhance the diffusive processes between impacts. Neither of these are completely satisfactory since in the first case diffusive events are missed and in the second case they can occur in the wrong order compared to what happens at a lower temperature.

Recently however there have been significant advances in long time scale dynamics which enable the calculation of these diffusive processes more quickly than by MD. Temperature accelerated dynamics allows for a correction of events that occur in the wrong order when the system is artificially heated (Sørensen, and Voter 2000). Other methods basically fall into two categories; those that bias the potential, to lower the energy barriers between adjacent minima but in such a way that the relative escape rates are not biased, e.g. the hyperdynamics (Voter 1997, Fichthorn and Miron 2009) and metadynamics (Laio and Parinello 2002) methods and those that search directly for (all) the saddle points surrounding a local minimum (metastable state) (Barkema and Mousseau 1996, Henkelmann and Jønsson 1999).

In the latter case a list of possible transitions can be constructed and the system evolved according to the relative probabilities of the candidate events. This is the basic approach used in order to model sputtering of Au surfaces at realistic dose rates adopted here which has also had success in modelling thin film growth (Blackwell et al 2012). The multi time step method therefore combines MD, used for the initial ballistic collision of a particle with the surface, with

a kinetic Monte Carlo (otf-KMC) model (Henkelman and Jønsson 2001, Scott et al., 2011) where system transitions between atomic impacts are determined on-the-fly. The initial application of a combined MD-otf-KMC approach for surface growth was given in the paper by Henkelman and Jønsson but at that time computing power was not so advanced. As a result their simulations were carried out at the unrealistically large growth rate of 1 monolayer per millisecond on a system much smaller than ours and there were fewer transitions between impacts as in our paper for sputtering at experimental dose rates. However if the diffusion barriers are all very high then assuming no diffusion between impacts would be a good approximation whereas if all the barriers are very low there would be no time saving by using the otf-KMC approach. A proper examination of these barriers is therefore essential and a full MD-otf-KMC approach will help validate previous more approximate models of sputtering. A few preliminary results on the application of MD-otf-KMC to sputtering were included in the previous paper (Scott et al., 2011), but the primary purpose of that publication was to demonstrate the methodology rather than the full analysis that is presented here. For the simulations discussed below, sputtering by both Au and Ar atoms is investigated and two initial crystal surfaces are chosen. The first is the (0 1 0) surface and the second a high index surface with a similar orientation (3 11 0). The reason for this latter choice is that surface topography such as cones and etch pits have been reported on such high index bombarded surfaces close to a major crystallographic direction, (Whitton et al 1984). The paper will examine this facet formation and also compare the sputtered particle distributions with those obtained assuming each particle impacts a perfect crystal surface.

2. METHODOLOGY

Simulations were carried out using the Ackland EAM potential for Au (Ackland et al 1984), splined to the screened Coulomb ZBL potential (Ziegler et al 1985) for close interaction. The EAM potential is fitted to the experimentally measured cohesive energy of Au (3.8 eV), the elastic constants of Au and the pressure-volume dependence. The Ar atoms interact with Au with a purely repulsive ZBL potential but interact with each other with a Lennard-Jones potential which allows some weak binding. The parameters for this are taken from Ashcroft and Mermin, 1976. This Lennard Jones potential is also splined to the screened Coulomb ZBL potential for close particle separation. Periodic boundary conditions in the lateral directions

were employed for the substrate. Various system sizes were considered, containing between 8,000 and 13,500 atoms whose surface areas were approximately 4nm x 4nm. Four sets of simulations were carried out for Ar and Au normal bombardment at 500 eV on the (0 1 0) and (3 11 0) oriented Au surfaces. The simulations started by first running MD for 20 ps with a 500 eV Au or Ar atom impact. The system was then relaxed and diffusion was simulated using otf-KMC. At each step either an impact event or a diffusion event is chosen, according to their relative probabilities. Erosion continued in this way until the required dose was reached. Most ballistic rearrangement at the bombardment energy of 500 eV takes place within the first 10 ps but the MD calculations are always faster than the saddle point searches so 20 ps did not involve excessive computation and also allowed some low energy barrier diffusion events to occur during the MD phase. The technique involves MD and otf-KMC working together in parallel over typically 24 or 48 cpu cores, where the impact event (MD) runs on a single core and searches are employed on multiple cores. A schematic of the process is given in Fig. 1. The saddle point searches are the most time consuming part of the calculation and the processor that carries out the MD calculation continues with saddle point searches once the MD calculation has been completed. The method works well when the energy barriers for diffusion between impacts are large enough that defects evolve only slowly compared to MD time scales. If this is not the case then the boost compared to MD alone can be quite modest. By 'boost' we mean the speed of using the otf-KMC approach compared to running MD alone. It will be seen later that for the Au impacts this criterion is satisfied but the simulations run slower for the Ar impacts due to sub-surface Ar diffusion events which have low barriers.

2.1. Molecular Dynamics

An impacting particle was placed in a random position a fixed height above the lattice, far enough away that there was initially no interaction between the incoming ion and the substrate. All impacts were performed normal to the surface (the $y-$ direction) at 500 eV. Periodic boundaries were applied in the x and z directions while the bottom layers of the system were held fixed and a thermostat used for the next three layers. Before each impact the entire substrate was heated to a temperature of 350 K. During the deposition the temperature of the thermal layers was held at 350 K.

2.2. On-the-fly Kinetic Monte Carlo

The otf-KMC algorithm involves four fundamental steps, described below:

1. Identify all the defects by comparison to a perfect bulk lattice. This produces a defect volume where defects and their neighbouring atoms are included. This defines the search space for a transition and typically contained about 600-700 atoms, much smaller than the full system used for the MD.

2. Search for all possible transitions. Locate saddle points by a direct search method starting from a random set of initial displacements from the local minimum (Vernon, 2010, Barkema and Mousseau 1996, Henkelmann and Jønsson 1999) and then use the climbing image Nudged Elastic Band method (Henkelmann et al 2000) to determine transition energy barrier heights E_b more accurately once the transition has been found. Typically 200 searches are carried out per KMC step.

3. Calculate the transition frequency ν using $\nu = \nu_0 \exp(-E_b/(kT))$, where k is Boltzmann's constant, T is temperature and ν_0 a prefactor, here assumed constant after some initial tests (3 cases only) showed that it varied by about 1 order of magnitude for most transitions. In addition rank 2 saddles had to be dealt with as a special case. To calculate the prefactor accurately (Vineyard, 1956) is time consuming and here a standard value of $10^{13}\mathrm{s}^{-1}$ was chosen. We expect that this prefactor will be more accurately determined in future versions of the code.

4. Transition searches together with a single particle impact event are carried out in parallel where the impact event runs MD on a single core and searches are employed on multiple cores. Either a transition or an impact event is chosen depending on their relative probability of occurrence after which the system evolves on an event driven basis.

A flux of between 2.3 and 2.6×10^{15} ions cm^{-2} s^{-1} was used to determine the rate (and therefore probability) of an impact event occurring. At 350 K this meant the deposition on the model substrate had the same probability as a transition with a barrier energy of ≈ 0.8 eV. Transition barriers greater than 1 eV are few and are discarded, since they are unlikely to be accessible within the relevant time scale for the impact event and chosen temperature; the ion impact is more than 1,000 times more likely to occur than a transition with a 1 eV barrier. The reason for the choice of 200 searches per step was because of the trade off between computational efficiency and the chances of missing an important transition. Typically we could

calculate 20 steps per day on 24 processors (Intel Westmere Xeon X5650 running at 2.66 GHz). We performed about 1000 steps for each simulation giving about 50 days computing in total. We have since improved the algorithm which reduces the saddle point search time considerably.

3. RESULTS

We first examine some of the events that can occur between impacts for the four sets of simulations that were carried out. With the estimated prefactor of $10^{13}\mathrm{s}^{-1}$, an energy barrier of ≈ 0.2 eV would correspond to a transition every 100 ps at 350 K; at 0.1 eV the transition would occur about every 3 ps. Since the barrier searches are also time consuming for a large boost compared to MD, it is important that most of the barriers lie in excess of this latter value otherwise the boost would be quite small. The distribution of transition energy barriers for diffusion between impacts for the Au on Au simulation is shown in Fig. 2a. This figure is a compendium of all barriers found throughout the simulation and within statistical accuracy has the same shape for both the (0 1 0) and (3 11 0) surfaces. Fig. 2a shows very few barriers above 0.85 eV and only a small number at low energies (< 0.2 eV), with the peak number of barriers occurring between 0.2 and 0.25 eV. The majority of the rest of the transition barriers fall between 0.4 and 0.65 eV with a mean transition barrier of 0.4 eV. Fig 2b shows the same combined results for the Ar bombardment. Now about 45% of barriers are 0.1 eV or less and these are almost entirely due to the diffusion of subsurface Ar atoms. This means that the Ar bombardment simulations run slower than those for Au but still with a substantial boost factor over MD. The calculated barrier distributions indicate that diffusion events between impacts would be important. If the barriers calculated were high then the ballistic effects induced by ion bombardment would dominate. If the barriers were too small then the KMC methodology would not allow significant boost. In the case of Ar bombardment, there are low energy barriers but the boost is still significant since the Ar diffuses out of the system and the low barriers are not always dominant. Fig. 2c shows the full set of energy barriers calculated for the Au on Au calculations, showing that larger barriers exist but they have a small probability of being chosen.

The peak at around 0.2 eV in Fig 2a comes from a wide variety of different transitions mainly involving single atom diffusion such as a single atom hop over the surface or the dropping down

of a single Au adatom at an edge to a lower level of the surface (Ehrlich-Schwoebel barrier). However some concerted motions also fall into this category, an example being when 3 subsurface Au interstitial atoms rotate and diffuse. Since there are so many possible different transitions a complete list is not given. A further transition was also calculated which was the barrier for a surface atom to jump from a lattice site in a perfect crystal to an adatom position. This is the event that would be dominant in a temperature-induced surface roughening process. This event was found to have a barrier of 1.54 eV and was never observed during the simulations. The reason for this is that if we assume a standard value for the prefactor, such a transition would occur on average every 9 days in our system, i.e. it is a very unlikely event. Thus the surface roughening that occurs is due entirely to the ballistic impacts and not to any temperature induced effects.

Many of these motions involve processes whereby the surface damage induced during the impact event heals. There are many possible mechanisms by which this can occur and it is not possible to list all but three of these are illustrated in Fig. 3 for 1, 2 and 3 atom motions. In (a) and (b) a single atom drops down to a lower level with an energy barrier of 0.2 eV. In (c) and (d) two atoms move together to fill a vacancy in a subsurface layer with an energy barrier of 0.43 eV whereas a concerted 3 atom motion occurs with an energy barrier of 0.72 eV shown in (e) and (f). It is clearly seen from these examples that surface healing between impacts is an important process which helps smooth the surface and lower the surface energy. If the dose rates are too high then rougher surfaces would be created. Simulations carried out at higher energies (Scott, 2012) indicate that rough surfaces can form if surface diffusion between impacts is not considered. Taking this into account for thin film growth is absolutely crucial in modelling the correct surface morphology (Blackwell et al, 2012).

Besides surface diffusion interstitial clusters that form below the surface can also diffuse. The small subsurface interstitial loops are fairly mobile with a three atom loop being able to diffuse (a rotation plus translation) with an energy barrier of 0.23 eV and a five atom loop with a barrier of 0.58 eV as shown in Fig.4. Vacancies have higher energy barriers and most of the diffusion that occurs between impacts occurs as a result of atomic rearrangements on the surface and the diffusion of subsurface interstitials, not the movement of vacancies.

Fig. 5 illustrates the subsurface processes that take place during erosion for Ar bombardment with snapshots of the subsurface interstitials after various simulation times. For clarity the

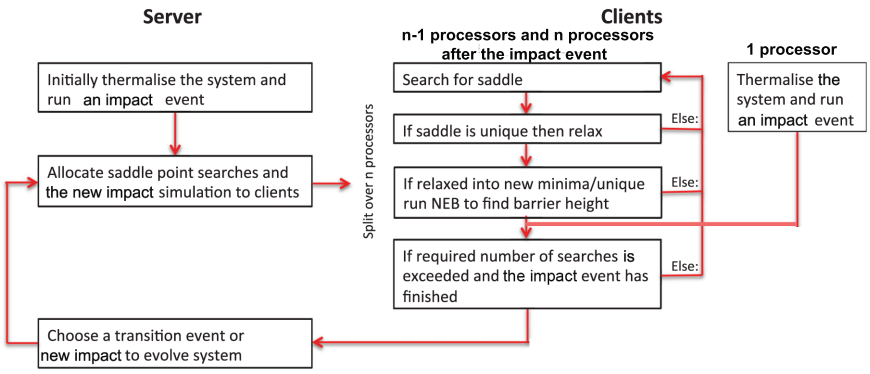

Figure 1: The client-server model that allows for the parallelisation of the sputter event and the searches for the transitions that occur between particle impacts.

subsurface vacancies are not shown. In (a) 0.075 s after the first impact there are adatoms lying above the height of the original Au surface, a four atom Ar cluster, a single Ar atom lying just below the surface and an eight atom interstitial loop. In (b) the interstitial loop has diffused and there has been rearrangement of the surface adatoms and the Ar cluster. Further rearrangement has occurred after 0.087s as shown in (c) where the Ar atom near the surface has diffused out and the interstitial cluster has recombined partially with subsurface vacancies. After 0.107s as shown in (d) a further impact has occurred. Some atoms have been sputtered from the surface, others rearranged into the existing craters and only 3 Ar atoms remain implanted. Thus surface erosion takes place due to a combination of sputtering and defect formation as a result of energetic single ion impacts together with diffusion and rearrangement of atoms between impacts. What is noticeable about the competition between the two processes is the remarkable amount of healing that takes place between impacts. Interstitial loops with up to 15 atoms were observed to form below the surface but eventually decay during subsequent bombardments. Analysis of the lifetime of the interstitial clusters showed that their lifetimes typically varied between 0.2×10^{-4} s and 0.2×10^{-2} s. The single interstitial and two atom cluster diffused and decayed between impacts whereas although the interstitial clusters containing between 4 and 10 atoms did diffuse, they were generally destroyed by a subsequent impact event. This suggest that the subsurface damage induced at 500 eV bombardment energy would also have healed if the simulations had been carried out using an artificially high dose rate as many MD simulations of

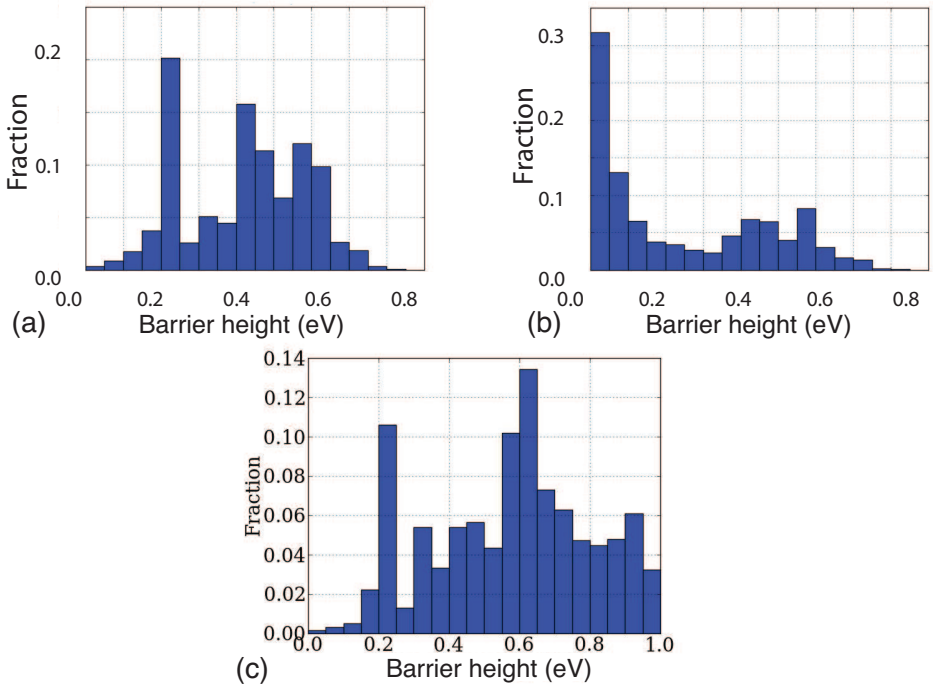

Figure 2: **(a)** The chosen transition energy barriers for diffusion between impacts for 500 eV Au normal incidence bombardment of Au. **(b)** The chosen transition energy barriers for diffusion between impacts for 500 eV Ar normal incidence bombardment of Au. (c) The full set of calculated barriers for the Au on Au calculations.

sputtering have done in the past. This would not be expected to be the case at higher energies where more and deeper damage would be created.

Sputtering yields measured experimentally have often had a different value from those calculated by modelling since the calculations in the past nearly always assumed a perfectly flat surface and did not take into account the roughening that occurs during the erosion process. Despite this, MD simulations have been successful in predicting a number of important quantities such as crater formation, the energy and angular distributions of the ejected atoms, (Webb and Harrison, 1983, Smith and Harrison, 1989, Lane et al, 2012). This is because sputtering by low energy ion impact (rather than cluster impact) is a fast process which occurs during the first few picoseconds after impact and therefore accessible computationally. One of the more interesting discoveries from the early MD simulations of sputtering was that the average sputter yield is determined from data taken from a large number of individual trajectories, some

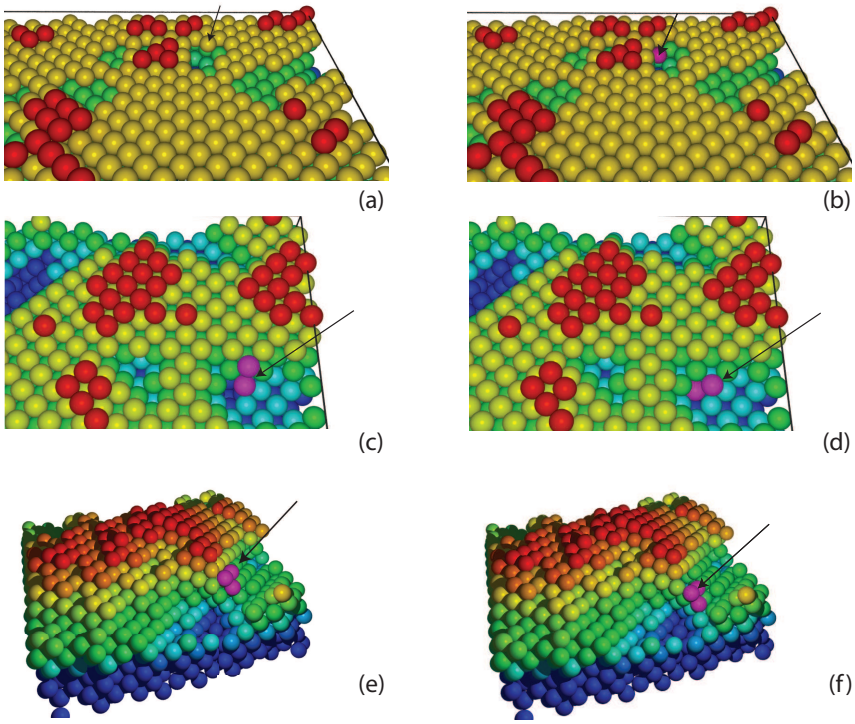

Figure 3: Examples of 'healing' transitions that occur on the Au surface between impacts, **(a)** and **(b)**: Single atom movement with barrier 0.2 eV, **(c)** and **(d)**: Concerted two atom motion with 0.43 eV barrier, **(e)** and **(f)**: Three atoms slide to a lower level on the surface with an energy barrier of 0.72 eV.

of which emit large numbers of particles and others that channel into the crystal. This trend increases as the energy of the impacting particle increases.

Fig. 6a shows the distribution of atoms per single impact data for the Ar atoms. The distribution is similar to that obtained from perfect crystalline surfaces; 9% of the incoming ions were reflected from the surface and in just under 14% of the impacts no atoms are sputtered. The mode of the distribution is 2, which happens in 16.7% of the cases. The maximum number of atoms sputtered per incoming ion was 18 and this occurred only once.

The kinetic energy distribution of the ejected particles shown in Figs. 6b and 6c shows some slight differences between the Ar and Au bombardments. In the case of Ar bombardment the maximum lies between 0 and 1 eV whereas for Au there is a peak between 1 and 2 eV. Fig. 6d shows the distribution obtained from Au bombardment of a perfect crystal surface and here we see the maximum in the distribution between 1 and 2 eV. The maximum in both figures lies in the region of half the cohesive energy (3.8 eV) of the substrate in agreement with Sigmund-

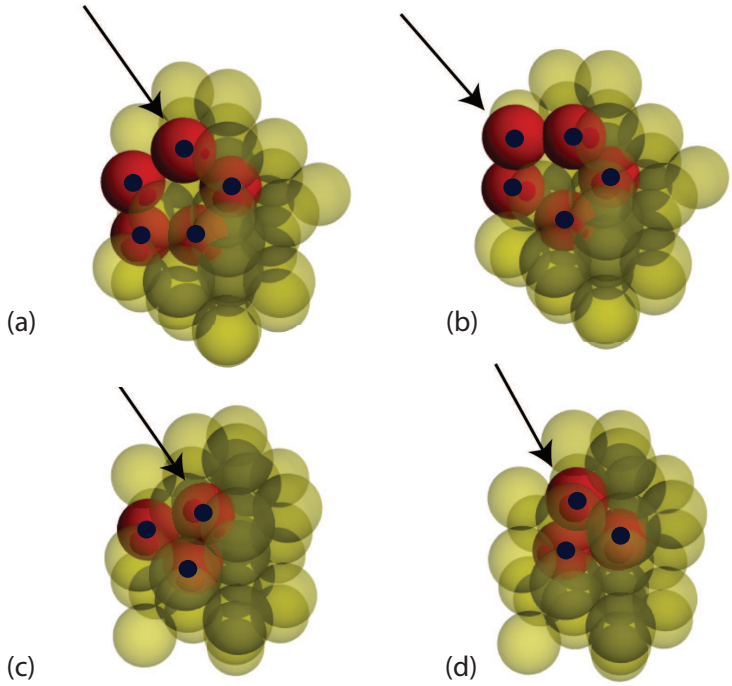

Figure 4: Examples of subsurface defect motion; (a) and (b) the rotation and translation of a 5 atom subsurface interstitial loop, with an energy barrier of 0.58 eV; (c) and (d) the rotation and translation of a subsurface 3 atom loop with an energy barrier of 0.23 eV. The arrows indicate the same atoms.

Thompson theory. The results for the perfect crystal also show a smaller peak and a less spread than for the multiply bombarded surface.

The value for the calculated sputtering yield varied between 3.2±0.2 atoms per ion for Au on the Au (0 1 0) surface to 3.4±0.2 for Ar. We also carried out some sputtering yield calculations assuming a perfectly flat crystal surface between impacts. The corresponding values were 3.1±0.1 and 3.5±0.1. These are the same within statistical error and a little higher than the experimentally observed sputtering yield of about 3 atoms per incident ion for both Au and Ar bombardment, (Andersen and Bay, 1981). Such yields are difficult to measure with accuracy and most experiments were carried out in the 1960s and 1970s. The original data by Oechsner (Oechsner, 1973) for example, has measured yields for 1 keV Ar bombardment that vary between 3 and 4. Also, data by Haywood and Wolter, (Haywood and Wolter, 1969) shows very little difference in measured yields between Ar and Au bombardment. Thus only 1 figure accuracy can be attributed to the experimentally measured sputtering yields.

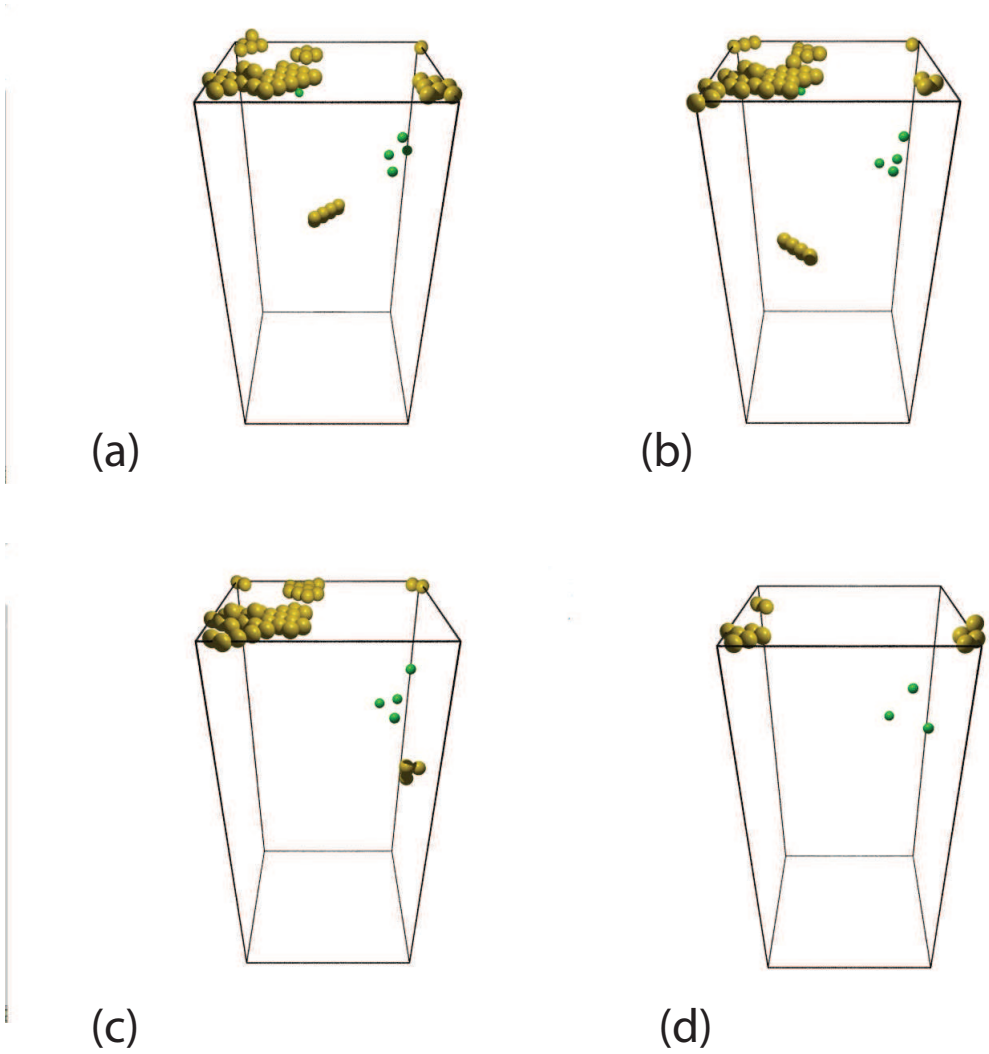

Figure 5: Snapshots of the erosion process for the Ar on Au (0 1 0) simulations, where only subsurface interstitial atoms are shown together with adatoms above the height of the original surface and the implanted Ar atoms. For clarity craters and vacancies are not shown. This illustrates the continual formation and decay of sub-surface interstitial loops **(a)** 0.075s; **(b)** 0.085s; **(c)** 0.087s; **(d)** 0.107s;

Figure 7 shows the final surface for Au bombardment of both the (0 1 0) and (3 11 0) surfaces. For the (0 1 0) surface the simulation was carried out for 3098 steps corresponding to 0.854s of real time. During this time the substrate was bombarded by 431 Au atoms, equivalent to a dose of 2.6×10^{15} atoms/cm^2. For the (3 11 0) surface which had a slightly different area, 2696 KMC steps were completed for a simulated time of 0.847 seconds. During this time 476 Au atoms bombarded the surface, a dose of $\approx 2.3 \times 10^{15}$ Au atoms/cm^2. The height difference between

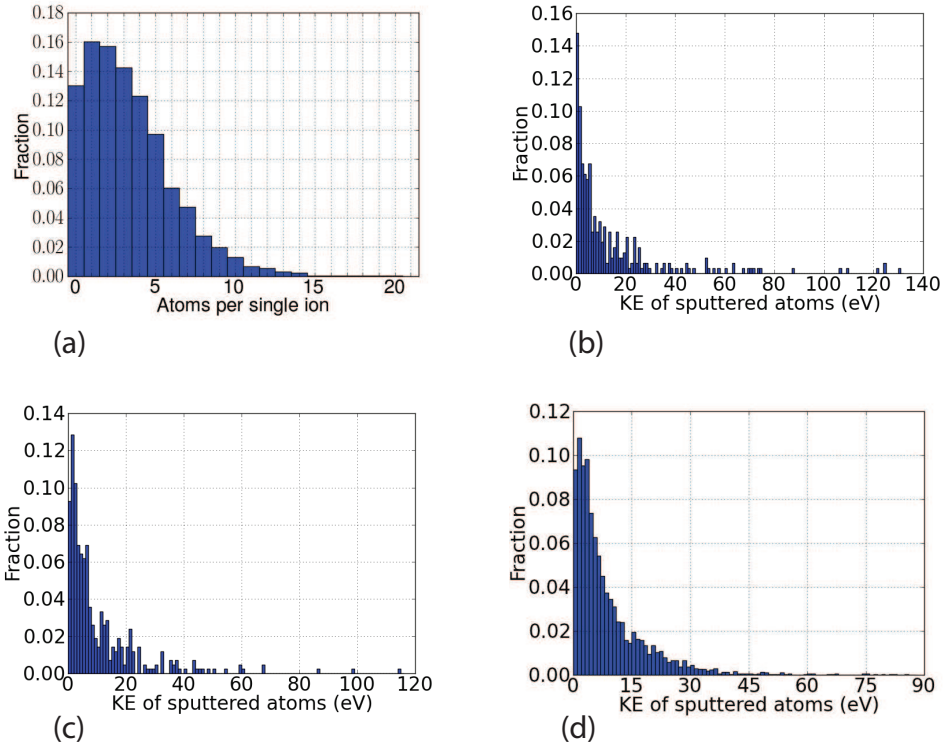

Figure 6: The atoms ejected per single ion impact (a) and the kinetic energy distributions of the ejected particles for the (010) surface after Ar impacts at 500eV (b). Figures (c) and (d) show the kinetic energy distributions of the ejected Au atoms after Au impacts at 500 eV. In (d) the simulation was carried out by assuming a perfect surface between each impact.

the exposed parts of the crystal is 2 nm on the (3 11 0) surface compared to only 1.2 nm on the (0 1 0) surface. In addition there is some evidence that low index facets are beginning to form on the (3 11 0) surface so there is a hint that the high index crystal surface is less stable. However the surface areas and fluxes used are too small to draw any firm conclusions concerning the development of large area topographical features such as those observed experimentally at higher doses and energies.

To investigate this further, Fig. 8 shows the average height of the surface against time for Ar bombardment on the (3 11 0) surface, while the root mean square surface roughness is plotted in Fig. 8(b). The initial height of the surface was 6.9 nm and the final average height, after 1.22 s, was 4.78 nm. This is an erosion rate of 1.74 nm/s. The surface height appears to drop nearly linearly as time progresses, a characteristic of the other impacts also.

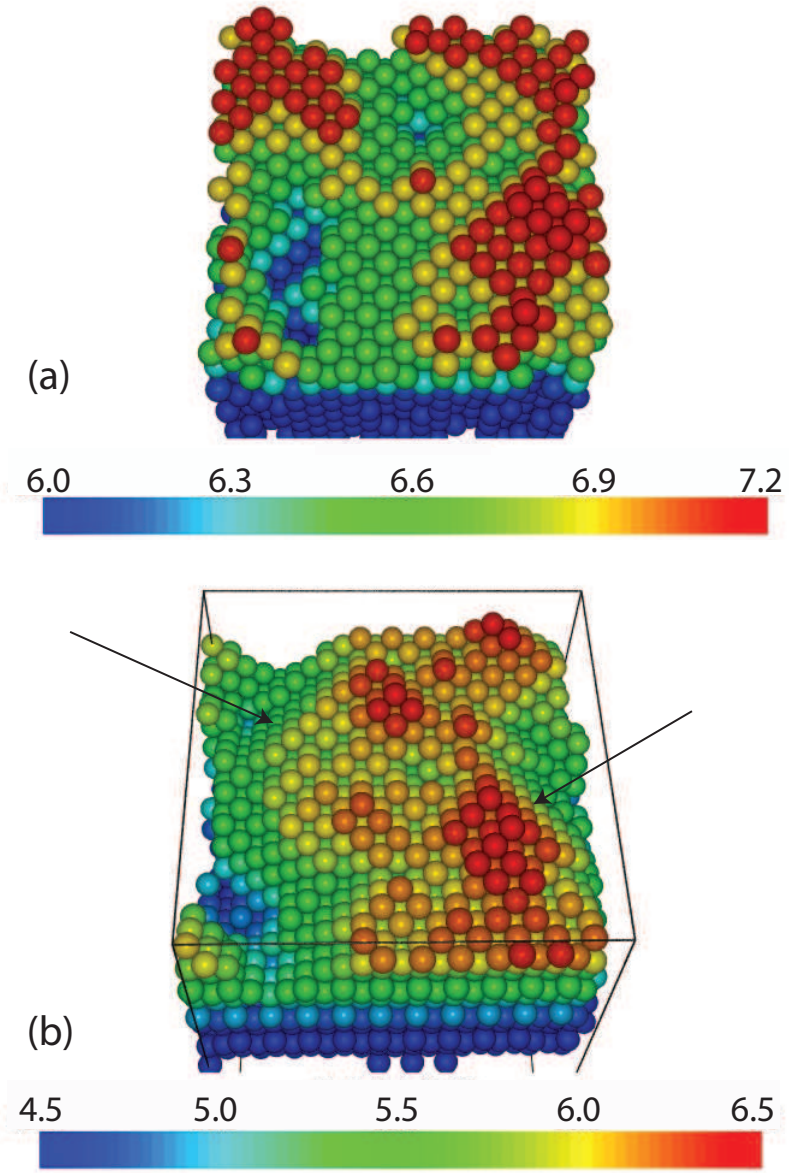

Figure 7: Snapshots of the final topography for the (0 1 0) (a) and (3 11 0), (b) surfaces after bombardment by Au atoms at 500 eV. The colour scheme refers to the height measured in nanometres from the reference level at the bottom of the simulation cell. The arrows in (b) mark the low index facets.

The surface roughness increases initially, then oscillates between approximately 0.2 and 0.4 nm, before increasing towards the end of the simulation up to around 0.5 nm. Again the results are somewhat inconclusive as to whether the surface is continuing to roughen or not. Ideally

to clarify this point, the simulation should be repeated on a larger system and for longer times when computing power becomes available.

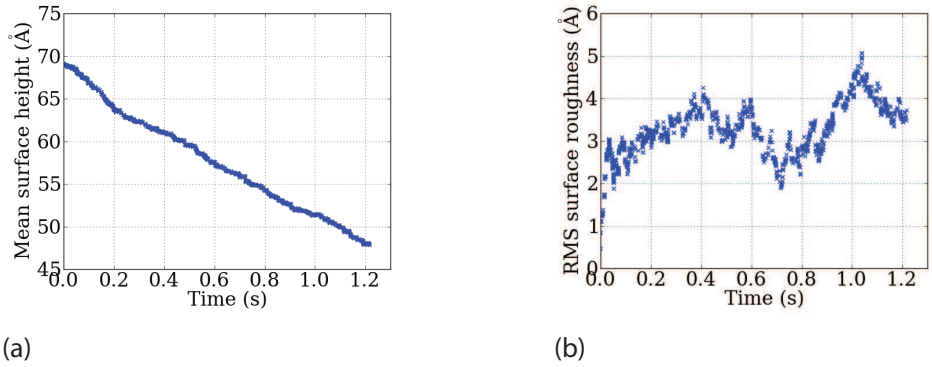

Figure 8: **(a)** The average height plotted as a function of time for Ar on Au bombardment of the (3 11 0) surface; **(b)** the corresponding RMS roughness of the surface.

4. CONCLUSION

A methodology is presented that enables the atomistic modelling of sputtering over realistic time scales with particular reference to 500 eV bombardment of gold. The method is to date limited to relatively small system sizes due to the computationally intensive process of saddle point searching in $3N$ dimensions. Currently work is under way to improve the search process so that as the software develops and as computers continue to increase in power, the method will have increasing application allowing simulations of larger systems. This would enable a clearer understanding of the topography development which for the relatively small surface area used in the paper, is limited by the periodic boundary conditions. A possible way to overcome this is to adopt the parallelisation methodology used to extend the temperature accelerated dynamics method, (Shim et al, 2007). Without this extension, we cannot be completely sure of the eventual scale of the surface topography that we have observed to develop on the high index surface (low index facet formation). Larger systems and higher doses need to be considered to investigate this fully. The methodology is also applicable to the investigation of surface roughening due to temperature effects alone. A systematic investigation of this effect as a

function of temperature has not been carried out due to the large amounts of computing time involved.

The sputtering yields, kinetic energy distributions of sputtered particles and the atoms per single ion distributions determined with the new method are in close agreement with data obtained from simulations on perfect crystal surfaces and the sputter yield calculations are close to experimentally measured values. In the case of the multiply bombarded surface the kinetic energy distribution has a longer tail compared to the perfect crystal but generally the work has confirmed that distributions obtained from perfect crystal surfaces are an excellent approximation. This is due to the remarkable amount of sub-surface healing that takes place between impacts so that the basic crystallinity of the substrate is maintained.

The formation of sub-surface defects by MD has previously been investigated by many authors, see for example Smith, King and Beardmore, 1997 and the evolution of sub-surface defects by long time scale dynamics (Uberuaga et al. 2005). The combination of the two approaches allows the examination of the relative rate of defect production and recombination to be studied. The methodology has shown that 1 or two atom sub-surface interstitials recombine with nearby vacancies or diffuse to the surface between impacts but that larger interstitial clusters decay as a result of further impacts. Thus subsurface damage does not accumulate at experimental dose rates and energies of 500 eV. This recovery process would not necessarily be expected to be the case for higher impact energies where deeper, larger less mobile defect clusters would be less accessible to annealing through further ballistic impact.

For the relatively small impact energy considered here, surface topography does develop with dose, even if the subsurface defect recovery process is dominant. In this case surface diffusion between impacts has a smoothing effect where surface atoms rearrange into lower energy sites. It is this process whereby facet formation can occur. Such facets were evident on the high index surface close to a major axis but our substrate was too small to determine the extent of this and how it would grow over time.

Although we have used the methodology to study surface and sub-surface damage due to sputtering, there are also many potential applications of the methodology in radiation damage studies both in the reactor core and also in the structural materials of the reactor where the atoms in the material are subjected to a large number of displacements and where well-separated large interstitial loops and vacancy clusters can form and not recombine.

The method has a wider application than just for the two-species problem discussed here and could be used in a number of different areas such as in fusion where low energy H and He atoms bombard the tungsten diverter causing fuzz formation. This problem has been studied by MD but only at unrealistic high dose rates which does not allow sufficient time between impacts for diffusion to occur. A further potential application is in thin film growth by using magnetron sputtering (Blackwell et al., 2012) where the species arrival rate is often time dependent. The methodology means that it is possible to distinguish between pulsed and RF sputtering since the fluence rates are easily incorporated into the model. The main points for successful application of the method are to have good potential energy functions that describe the system and that the diffusion is not dominated by low energy barriers.

Acknowledgements

The authors would like to thank Louis Vernon and Steven Kenny for useful discussions. The work was also supported by an EPSRC funded studentship.

References

Ackland, G. J., Tichy, G., Vitek, V. & Finnis, M. W. 1987 Simple N-body potential for the noble metals and nickel. *Phil. Mag A* **56** 735-756.

Ashcroft, N.W. and Mermin, N.D. 1976 *Solid State Physics* pp 398 Fort Worth, Saunders College Publishing.

Behrisch, R. 1981 *Sputtering by Particle Bombardment* vol.1 and 2 Berlin, Springer-Verlag.

Andersen, H. H & Bay, H. L. 1981 Sputtering yield measurements. In *Sputtering by Particle Bombardment I*, (ed. R. Behrisch), vol.1, pp.145-218. Berlin, Springer-Verlag.

Barkema, G. T. & Mousseau, N. 1996 Event-based relaxation of continuous disordered systems. *Phys. Rev. Lett.* **77** 4358-4361.

Blackwell, S, Smith, R. Kenny, S. D., Walls, J. M. & Vernon, L. J. 2012 Modeling evaporation, ion beam assist and magnetron sputtering of thin metal films over realistic time scales. *Phys. Rev. B* **86** 035416.

Domain, C., Becquart, C. S. & Malerba, L. 2004 Simulation of radiation damage in Fe alloys : an object kinetic Monte Carlo approach. *J. Nucl. Mater.* **335** 121-145.

Fichthorn, K. A. & Miron, R. A. 2009 Accelerated Molecular-Dynamics Simulation of Thin

Film Growth. *Computer Simulation in Condensed Matter Physics XIX, Springer Proceedings in Physics* **123** 7-16.

Goldman, D.T., Harrison, D. E. & Coveyou, R. R. 1959, A Monte-Carlo calculation of high energy sputtering. *Tech. Rpt. ONRL-2729*, Oak Ridge.

Grove, W. R. 1852 On the electro chemical polarity of gases. *Phil. Trans. R. Soc. London* **142** 87-101.

Harrison, D. E. 1960 Extended theory of sputtering. *J. Chem Phys.* **32** 1336-1341.

Harrison, D. E., Johnson, J. P., & Levy, N. S. 1966 Spot patterns and Silsbee chains on a Cu single crystal. *Appl. Phys. Lett.* **8** 33-36.

Haywood, W. H. and Wolter, A. R. 1969 Sputtering Yield Measurements with Low-Energy Metal Ion Beams *J. Appl. Phys.* **40** 2911-2916.

Henkelman, G. & Jønsson, H. 1999 A dimer method for finding saddle points on high dimensional potential surfaces using only first derivatives. *J. Chem. Phys.* **111** 7010-7014.

Henkelman, G. & Jønsson, H. 2001 Long time scale kinetic Monte Carlo simulations without lattice approximation and predefined event table. *J. Chem. Phys* **115** 9657-9666.

Henkelman, G, Uberuaga, B. P. & Jønsson, H. 2000 A climbing image nudged elastic band method for finding saddle points and minimum energy path. *J. Chem. Phys.* **113** 9901-9905.

Laio, A. & Parrinello, M. 2002 Escaping free energy minima. *Proc. Nat. Acad. Sci. USA*, **99** 12562-12566.

Lane, P.D., Galloway, G.J., Cole, R.J, Caffio, M. Schaub, R. & Ackland, G.J. 2012 Validating molecular dynamics with direct imaging of radiation damage debris *Phys. Rev. B* **85** 094111.

Oechsner, H. 1973 Untersuchungen zur Festkörperzerstübung bei schiefwinkligem Ionenbeschulßpolykristalliner Metalloberflächen im Energiebereich um 1 keV Z. Phys. **261** 37-58.

Postawa, Z., Czerwinski, B., Winograd, N. & Garrison, B. J. 2005 Microscopic Insights into the sputtering of thin organic films on Ag(111) by C_{60} and Ga Bombardment. *J. Phys. Chem. B* **109** 11973-11979.

Scott, C., Blackwell, S, Vernon, L. J. , Kenny, S. D., Walls, J. M. & Smith, R. 2011 *J. Chem. Phys.* **135** 174706.

Scott, C., 2012 A computational study of surface topography arising from energetic particle interactions *PhD. thesis Loughborough University.*

Shim, Y., Amar, J.G., Uberuaga, B.P., & Voter, A.F. 2007 Reaching extended length and time-scales via parallel temperature-accelerated dynamics, *Phys. Rev. B* **76** 205439.

Sigmund, P. 1969 Theory of sputtering I : Sputtering yield of amorphous and polycrystalline targets. *Phys. Rev.* **184** 383-395.

Sørensen, M. R. & Voter, A. F. 2000 Temperature-accelerated dynamics for simulation of infrequent events. *J. Chem. Phys.* **112** 9599-9607.

Smith, R. & Harrison, D. E. 1989 High yield sputtering events for Ar bombardment of Cu in the energy range 1-20 keV. *Phys. Rev. B* **40** 2090-2096.

Smith, R. King, B & Beardmore, K 1997 Molecular dynamics simulation of 0.1-2 keV ion bombardment of Ni100 *Rad. Eff. and defects in Solids* **141** 425-451

Thompson, M. W. 1968 Energy spectrum of ejected atoms during high-energy sputtering of gold. *Phil. Mag.* **18** 377-414.

Thompson, M. W. , Colligon, J. S. & R. Smith, R. 2004 Sputtering, past present and future. *Phil. Trans. Roy. Soc.* **362**.

Uberuaga, B. P., Smith, R., Cleave, A. R., Henkelman, G,. Grime, R.W., Voter, A. F. & Sickafus, K.E (2005) *Dynamical simulations of radiation damage and defect mobility in MgO Phys. Rev. B* **71** 104102.

Vernon, L. J. 2010 Modelling the growth of TiO_2. PhD thesis, Loughborough University.

Vineyard, G. H. 1957 Frequency factors and isotope effects in solid state rate processes. *J. Phys. and Chem. Solids* **3** 121-127.

Voter, A. F. 1997 Hyperdynamics: Accelerated molecular dynamics of infrequent events. *Phys. Rev. Lett.* **78** 3908-3911.

Webb, R. P & Harrison, D. E. 1983 Computer simulation of pit formation in metals by ion bombardment. *Phys. Rev. Lett.* **50** 1478-1481.

Webb, R. P., Garrison, B. J. & Vickerman, J. C. 2011 The effect of the H:C ratio on the sputtering of molecular solids by fullerenes. *Surf. and Interface. Anal.* **43** 116-119.

Whitton, J. L., Kiriakidis, G., Carter, G., Lewis, G. W. & Nobes, M. J. 1984 The development of sputter induced pits and pyramids on ion bombarded (11 3 1) surfaces of fcc cubic single crystals. *Nucl. Instrum and Meth. B.* **2** 640-644.

Yastrebov, S. & Smith, R. 2001 Growth of amorphous carbon films by carbon atom bombardment in the energy range 10-500 eV. *Nucl. Instrum. and Meth. B* **180**, 145-152.

Ziegler, J. F., Biersack, J. P. & Littmark, U., 1985 *The Stopping and Range of Ions in Solids*, pp 107-110 New York: Pergamon.